Ubiquitin ligase Triad1 promotes neurite outgrowth by inhibiting MDM2-mediated ubiquitination of the neuroprotective factor pleiotrophin

Received for publication, March 21, 2022, and in revised form, August 18, 2022 Published, Papers in Press, August 31, 2022,
https://doi.org/10.1016/j.jbc.2022.102443

Chunshuai Wu[1,2,3], Guanhua Xu[1], Guofeng Bao[1], Hong Gao[1], Jiajia Chen[1], Jinlong Zhang[1], Chu Chen[1], Hongxiang Hong[1], Pengfei Xue[1], Jiawei Jiang[1], Yang Liu[1], Jiayi Huang[1], Yue Sun[1], Jiawei Fu[1], Yiqiu Li[1], and Zhiming Cui[1,2,3,*]

From the [1]Department of Spine Surgery, The Affiliated Hospital 2 of Nantong University, The First People's Hospital of Nantong, Nantong, China; [2]Key Laboratory for Restoration Mechanism and Clinical Translation of Spinal Cord Injury, Nantong, China; [3]Research Institute for Spine and Spinal Cord Disease of Nantong University, Nantong, China

Edited by Elizabeth Coulson

Spinal cord injury (SCI) is the most severe result of spine injury, but no effective therapy exists to treat SCI. We have previously shown that the E3 ubiquitin ligase Two RING fingers and DRIL 1 (Triad1) promotes neurite outgrowth after SCI. However, the mechanism by which Triad1 affects neuron growth and the potential involvement of its ubiquitination activity is unclear. Neuroprotective cytokine pleiotrophin (PTN) can promote microglia proliferation and neurotrophic factor secretion to achieve neuroprotection. We find using immunostaining and behavioral assays in rats that the expression of Triad1 and the PTN was peaked at 1 day after SCI and Triad1 improved motor function and histomorphological injury after SCI. We show using flow cytometry and astrocyte/neuronal coculture assays that Triad1 overexpression promoted PTN protein levels, neurotrophic growth factor (NGF) expression, brain-derived neurotrophic factor (BDNF) expression, astrocyte and neuronal viability, and neurite outgrowth but suppressed astrocyte apoptosis, while shRNA-mediated knockdown of Triad1 and PTN had the opposite effects. Ubiquitin ligase murine double mutant 2 (MDM2) has previously been demonstrated to participate in the process of neurite outgrowth and mediate ubiquitination of p53. Furthermore, we demonstrate overexpression of MDM2 downregulated PTN protein levels, NGF expression and BDNF expression in astrocytes, and inhibited neurite outgrowth of neurons. In addition, MDM2 facilitated PTN ubiquitination, which was reversed by Triad1. Finally, we show simultaneous sh-PTN and MDM2 overexpression attenuated the neurite outgrowth-promoting effect of Triad1 overexpression. In conclusion, we propose Triad1 promotes astrocyte-dependent neurite outgrowth to accelerate recovery after SCI by inhibiting MDM2-mediated PTN ubiquitination.

Spinal cord injury (SCI) is the damage to spinal canal nerve structure (including spinal cord and nerve root) caused by trauma, inflammation, tumors, and other pathogenic factors, further leading to spinal cord nerve dysfunction (1–3). After SCI, regenerated neurons are almost nonexistent so that the restoration of nerve function only depends on the remaining neurons. However, neurons possess limited abilities to grow neurite during the repair, and the utilization of growth factors and neurotrophic factors such as nerve growth factor (NGF) and brain-derived neurotrophic factor (BDNF) is insufficient (4–6). These two aspects, therefore, need to be improved for the functional recovery of patients with SCI.

Two RING fingers and DRIL 1 (Triad1), one of E3 ubiquitin ligases, is a critical member of RING Between RING-RING (RBR) family involved in assorted important intracellular events such as transcription, translation, posttranslational modification, and protein stability regulation (7, 8). A previous study demonstrated that Triad1 regulates membrane transport, and its mutants lead to improper accumulation of receptors like growth hormone receptor and epidermal growth factor receptor on the endosome and plasma membrane (9). In addition, it has been discovered in our previous research that Triad1 promotes the neurite outgrowth of neurons after SCI through regulating the expression of EHD1 (4). Nonetheless, the regulatory mechanism of Triad1 on neurite outgrowth needs more exploration, and whether the role of Triad1 in neurite outgrowth is associated with ubiquitination is also an unsolved mystery.

Ubiquitin is a highly conserved low molecular weight protein widely existing in eukaryotic cells (10). Ubiquitination refers to the process that ubiquitin molecules classify intracellular proteins under the action of a series of special enzymes, select target proteins, and modify target proteins with high specificity, so as to degrade specific signal proteins in cells with high selectivity (11, 12). As an important E3 ubiquitin ligase, Triad1 has previously been demonstrated to suppress murine double minute 2 (MDM2)–mediated ubiquitin-dependent degradation of p53 through binding to p53 (13, 14). Besides, the MDM2/p53/IGF1R axis enhances axonal sprouting and functional recovery after SCI in mice (15). What awaits to be expounded is that whether the inhibition of

* For correspondence: Zhiming Cui, zhimingcuispine@163.com.

Triad1 on MDM2-mediated ubiquitination is associated with the recovery progression. Interestingly, our research additionally revealed that there is an interaction between Triad1 and pleiotrophin (PTN), a kind of secretory neurotrophic factor that can promote microglia proliferation and neurotrophic factor secretion to achieve neuroprotection (16). Nevertheless, there is still a lack of research on whether the neuroprotection of PTN is related to Triad1.

Therefore, in this research, we established a SCI rat model and cultured primary rat astrocyte and neuron. The effects of Triad1, MDM2, and PTN on the astrocyte function, neurite outgrowth of neuron, and functional recovery after SCI were systematically investigated for the first time.

Results

Triad1, PTN, and MDM2 were highly expressed and interacted with each other in SCI rats

After the SCI rat model was established, the motor function of all rats was evaluated through Basso, Beattie, and Bresnahan (BBB) locomotion rating scale (Fig. 1*A*) and the inclined plane test (Fig. 1*B*). The results confirmed that the BBB score and incline angle of SCI rats were notably lower than those of rats receiving sham operation ($p < 0.001$), indicating the motor function of SCI rats was impaired. Subsequently, the histomorphological changes of injured spinal cord tissues at 7 days after surgery were then examined by H&E staining and Nissl staining. Images from H&E staining exhibited severe damage to central gray matter and dorsal white matter in SCI rats (Fig. 1*C*). As depicted in Figure 1, *D* and *E*, SCI induced severe neuronal loss when compared with sham operation ($p < 0.001$). Then, the expressions of MDM2, PTN, and Triad1 in spinal cord tissues at different time points were determined. The results reflected that the three gene expressions were all upregulated in SCI rats ($p < 0.001$, Fig. 1, *F–I*), of which MDM2 expression was the highest at 6 h (h) after surgery, while PTN and Triad1 expressions were upregulated at 12 h after SCI, peaked at 1 day and then declined gradually during the following days. The immunohistochemistry performed on spinal cord tissues at the first day after surgery verified that PTN-positive cells and Triad1-positive cells were increased in SCI rats (Fig. 2*A*). To preliminarily explore the association among MDM2, PTN, and Triad1, coimmunoprecipitation (Co-IP) was conducted using the protein of spinal cord tissues at the first day after surgery. As exhibited in Figure 2, *B* and *C*, Triad1 precipitated PTN with MDM2 (Fig. 2*B*) and PTN precipitated Triad1 with MDM2 (Fig. 2*C*). These results evidenced the interaction of Triad1, PTN, and MDM2 in SCI.

The expressions of Triad1, MDM2, and PTN were increased in neurons and in astrocytes following SCI

Triad1, MDM2, and PTN with NeuN and GFAP were double labeled on the transverse cryosections of rat spinal cords in the sham and SCI-1 day groups. Triad1, MDM2, and PTN were colocalized in neurons and astrocytes, and their expressions were increased at 1 day after SCI (Fig. S1).

Triad1 overexpression promoted the translation level of PTN and the expressions of NGF and BDNF in rat astrocytes

The primary neurons and astrocytes were identified *via* NeuN or GFAP immunofluorescent labeling (Fig. S2). The function of neurons can be supported by astrocytes (17). To investigate the mechanism of Triad1 in SCI, rat astrocytes and cortical neurons were cultured and a series of *in vitro* experiments were carried out. After Triad1 was overexpressed or silenced in astrocytes ($p < 0.001$, Fig. 3, *A* and *B*), the transcription and translation levels of PTN were then evaluated. Figure 3, *C* and *D* reflected that the translation level of PTN was promoted by Triad1 overexpression but was inhibited by Triad1 silencing ($p < 0.001$, Fig. 3*C*), accompanied by unaffected transcription level of PTN (Fig. 3*D*). In addition, overexpressed Triad1 unregulated while Triad1 silencing downregulated transcription and translation levels of NGF and BDNF ($p < 0.001$, Fig. 3, *E* and *F*), as well as the secretion levels of NGF and BDNF in culture supernatant of astrocytes ($p < 0.001$, Fig. 3*G*).

Triad1 overexpression enhanced the viability and inhibited the apoptosis of rat astrocytes to facilitate the neurite outgrowth in rat neurons by inhibiting PTN ubiquitination

The biological function of astrocytes was evaluated, with Figure 4, *A–C* depicting that upregulated Triad1 strengthened the viability ($p < 0.001$, Fig. 4*A*) and inhibited the apoptosis ($p < 0.05$, Fig. 4, *B* and *C*) of astrocytes, while downregulated Triad1 generated the opposite influences ($p < 0.001$, Figure 4*A*; $p < 0.001$, Fig. 4, *B* and *C*). After coculture of neurons and rat astrocytes transfected with plasmid overexpressing Triad1 or sh-Triad1, the results showed that the microtubule associated protein 2 (MAP2)–positive cells (Fig. 4*D*), neurite outgrowth (Fig. 4*E*), nerve bifurcation numbers (Fig. 4*F*), and viability (Fig. 4*G*) of rat neurons were promoted by upregulated Triad1 ($p < 0.001$) but were suppressed by downregulated Triad1 ($p < 0.01$). Furthermore, to verify whether Triad1 regulated the ubiquitination of PTN, Flag-PTN was cotransfected with His-Ub in the presence of Myc-Triad1 in HEK-293 cells. Data in Figure 4*H* reflected that PTN was strongly ubiquitinated in cells without Myc-Triad1, which was then suppressed by Myc-Triad1. Subsequently, astrocytes were cotransfected with Triad1 overexpression plasmid and sh-PTN. The expression of PTN was upregulated by Triad1 overexpression plasmid but was downregulated by sh-PTN ($p < 0.001$, Fig. 5*A*), while the effect of Triad1 overexpression plasmid on PTN expression could be reversed by sh-PTN ($p < 0.001$, Fig. 5*A*). Meanwhile, after coculture of rat astrocytes with neurons, the neurite outgrowth (Fig. 5*B*), nerve bifurcation numbers (Fig. 5*C*), and the MAP2-positive cells (Fig. 5*D*) in rat neurons were promoted by Triad1 upregulation ($p < 0.001$) but were inhibited by PTN downregulation ($p < 0.01$). Notably, PTN downregulation offset the effect of Triad1 overexpression ($p < 0.05$). All these results indicated that Triad1 overexpression inhibited PTN ubiquitination to promote the viability and inhibit the apoptosis of rat astrocytes, thus enhancing the neurite outgrowth in rat neurons.

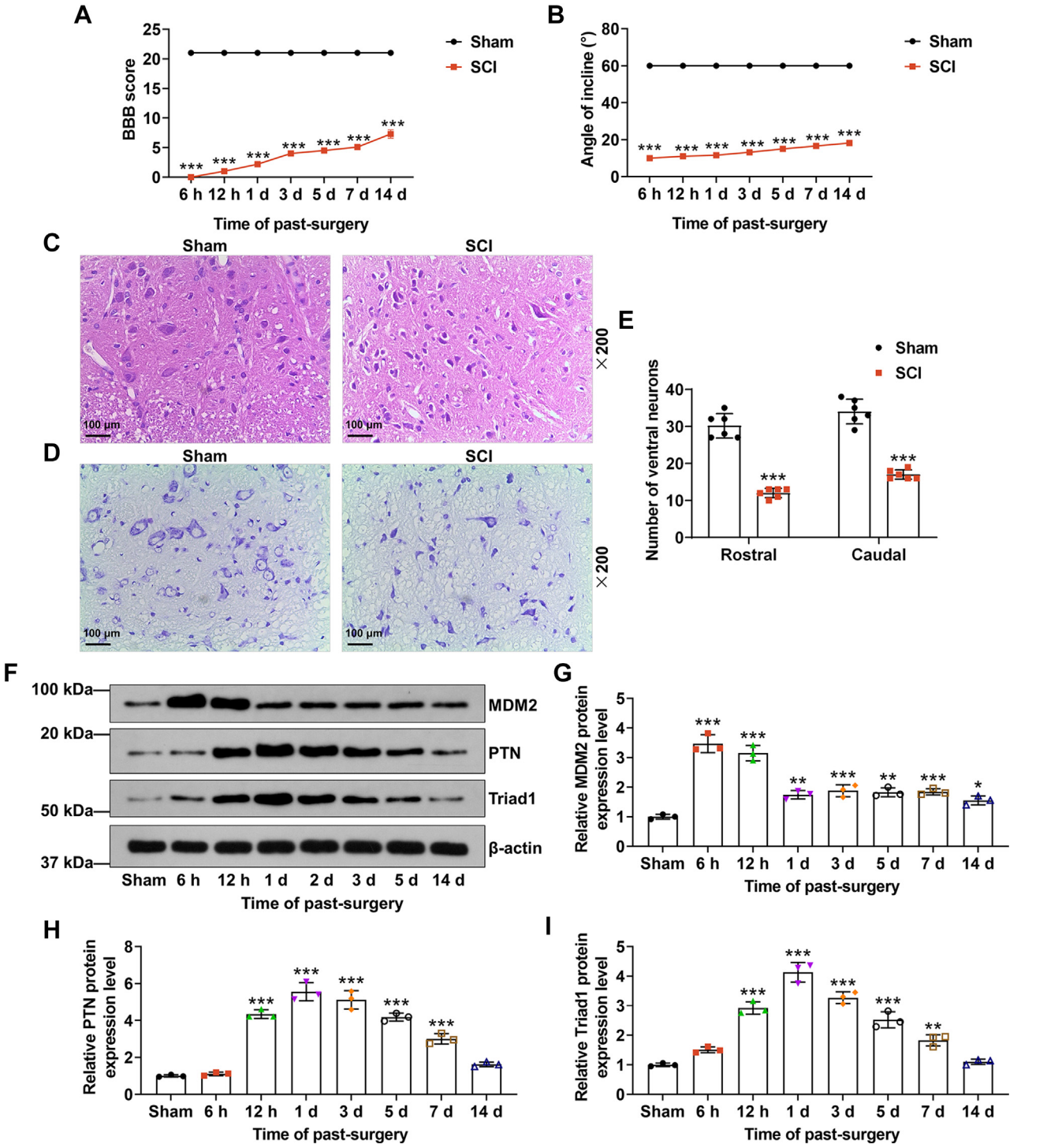

Figure 1. Triad1, PTN and MDM2 expressions were up-regulated in SCI rats. *A* and *B*, after the SCI rat model was established, the motor function of all rats was evaluated through BBB locomotion rating scale (*A*) and the inclined plane test (*B*). *C–E*, the histomorphological changes of injured spinal cord tissues at 7 days after surgery were then examined by H&E staining (*C*) and Nissl staining (*D*), and the number of ventral neurons was then calculated (*E*). Magnification: ×200; scale bars: 100 μm. *F–I*, the expressions of MDM2, PTN, and Triad1 in spinal cord tissues at different time points were determined through Western blot. (*$p < 0.05$, **$p < 0.01$, ***$p < 0.001$, *versus* sham). MDM2, murine double minute 2; PTN, pleiotrophin; SCI, spinal cord injury; Triad1, two RING fingers and DRIL 1.

MDM2 overexpression downregulated the translation level of PTN while MDM2 silencing did the opposite

UbiBrowser (http://ubibrowser.ncpsb.org/) was employed to further explore whether the E3 ligase mediates the PTN ubiquitination. The predicted interacting factors are arranged clockwise in descending order according to the confidence score. As exhibited in Figure 6*A*, MDM2 had the greatest possibility to regulate the PTN ubiquitination.

Therefore, the transcription and translation levels of PTN in rat astrocytes after MDM2 overexpression or silencing (Fig. 6, *B* and *C*) were evaluated. The results affirmed that only the translation level of PTN was suppressed by overexpressed MDM2 ($p < 0.001$, Fig. 6*C*) yet promoted by silenced MDM2 ($p < 0.001$, Fig. 6*C*).

Triad1 inhibited the MDM2-mediated PTN ubiquitination

The effect of MDM2 on PTN ubiquitination was then investigated by Co-IP. As indicated in Figures 7*A* and S3*A*, cotransfection with Flag-PTN, HA-MDM2, and His-Ub promoted the PTN ubiquitination in HEK-293 cells or astrocytes, relative to cotransfection with Flag-PTN and His-Ub. Since MG132 could block proteasome-mediated degradation of ubiquitin-conjugated proteins, it was further employed in Co-IP to verify the aforementioned discovery. The data in Figures 7*B* and S3*B* revealed that in the presence of MG132, PTN ubiquitination was promoted in the cells cotransfected with Flag-PTN and His-Ub in the presence or absence of HA-MDM2, demonstrating that MDM2 mediated PTN ubiquitination. To further prove that MDM2-mediated PTN ubiquitination could be regulated by Triad1, the expression and ubiquitination of PTN were evaluated. According to Figure 7*C*, the expression of PTN was diminished by MDM2 overexpression and elevated by Triad1 overexpression ($p < 0.001$), and MDM2 and Triad1 overexpression could reverse the effects of each other ($p < 0.001$). Also, the expression of Triad1 was downregulated by MDM2 overexpression ($p < 0.01$, Fig. 7*D*). After the Co-IP was performed again, the data revealed that in the presence of Myc-Triad1, the ubiquitination of PTN was weakened (Figs. 7*E* and S3*C*). All these findings demonstrated that Triad1 inhibited the MDM2-mediated PTN ubiquitination in rat astrocytes.

MDM2 overexpression attenuated the promoting effect of upregulated Triad1 on NGF and BDNF expressions in rat astrocytes and neurite outgrowth of rat neurons

The effect of MDM2 on rat astrocytes and neurons was analyzed. The protein and mRNA levels of NGF and BDNF in rat astrocytes were down-regulated by MDM2 overexpression but were up-regulated by Triad1 overexpression ($p < 0.001$, Fig. 8, *A* and *B*), whereas MDM2 overexpression further reduced the promoting effect of Triad1 overexpression on NGF and BDNF expressions ($p < 0.001$, Fig. 8, *A* and *B*). Correspondingly, the secretion of NGF and BDNF in culture supernatant of astrocytes also received the same effects from MDM2 and Triad1 overexpression ($p < 0.001$, Fig. 8*C*), and MDM2 overexpression similarly weakened the promoting effect of Triad1 overexpression on NGF and BDNF secretion ($p < 0.05$, Fig. 8*C*). After co-culture of rat astrocytes with neurons, the neurite outgrowth (Fig. 8*D*), never bifurcation numbers (Fig. 8*E*), and MAP2-positive cells (Fig. 8*F*) of rat neurons were suppressed by MDM2 overexpression ($p < 0.01$) but were promoted by Triad1 overexpression ($p < 0.001$), with MDM2 overexpression further impairing the effect of Triad1 overexpression ($p < 0.01$). These discoveries signified that the effects of Triad1 on rat astrocytes and neurite outgrowth of rat neurons were realized by regulating MDM2.

Triad1 improved the motor function and histomorphological injury of SCI rats

The role of Triad1 in SCI rats was verified *in vivo*. After the SCI rat model was established and pretreated with adenovirus containing Triad1 overexpression plasmid, the motor function of all rats was evaluated through BBB locomotion rating scale (Fig. 9*A*) and the inclined plane test (Fig. 9*B*). The data unveiled that the BBB score and incline angle of SCI rats were

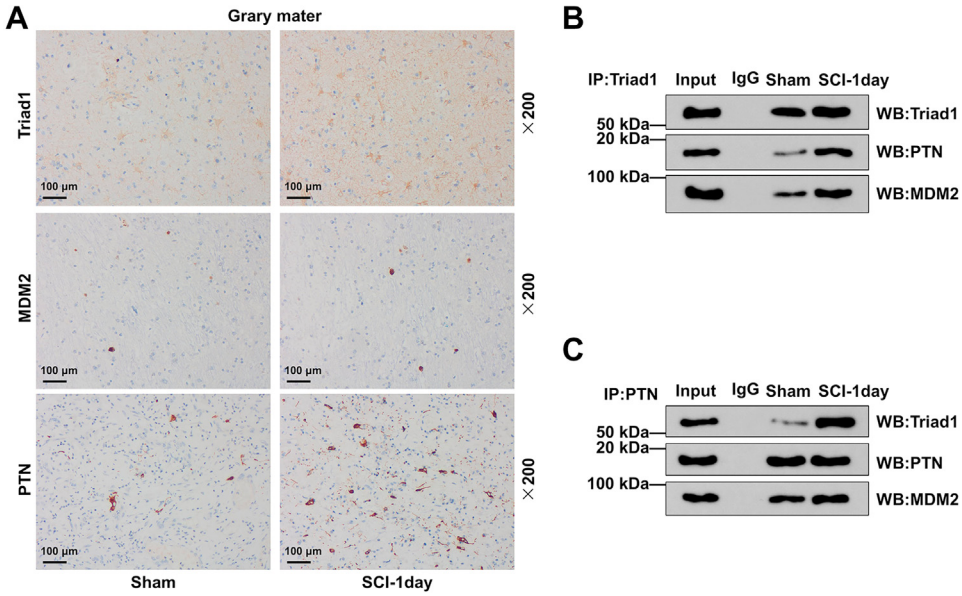

Figure 2. Triad1, PTN and MDM2 interacted with each other in SCI rats. *A*, Triad1-positive cells, MDM2-positive cells, and PTN-positive cells in spinal cord tissues at 1 day after surgery were detected through immunohistochemistry. Magnification: ×200; scale bars: 100 μm. *B* and *C*, Co-IP was performed to explore the association between MDM2, PTN, and Triad1 in spinal cord tissues at 1 day after surgery. Co-IP, coimmunoprecipitation; MDM2, murine double minute 2; PTN, pleiotrophin; SCI, spinal cord injury; Triad1, two RING fingers and DRIL 1.

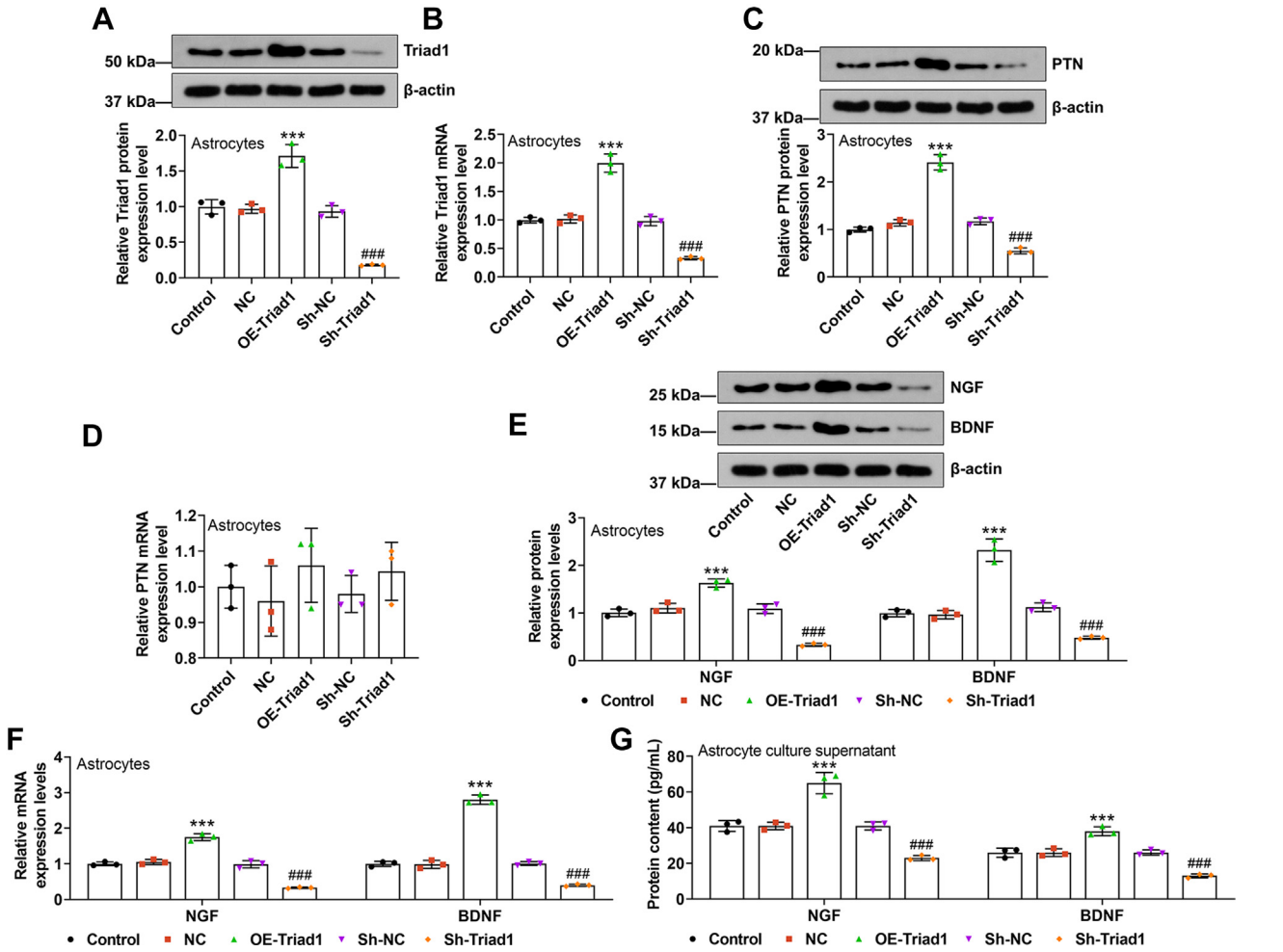

Figure 3. Triad1 overexpression promoted the translation level of PTN and the expressions of NGF and BDNF in rat astrocytes. *A* and *B*, after rat astrocytes were isolated and cultured, Triad1 was overexpressed or silenced in astrocytes through transfection, and detected by Western blot (*A*) and qRT-PCR (B). *C* and *D*, the transcription and translation levels of PTN in astrocytes after transfection were evaluated by Western blot (*C*) and qRT-PCR (*D*). *E* and *F*, the transcription and translation levels of NGF and BDNF in astrocytes after transfection were determined by Western blot (*E*) and qRT-PCR (*F*). *G*, the secretion of NGF and BDNF in culture supernatant of astrocytes was evaluated by ELISA. (***$p < 0.001$, *versus* NC; ###$p < 0.001$, *versus* sh-NC). BDNF, brain-derived neurotrophic factor; NC, negative control; NGF, nerve growth factor; OE, overexpressed; PTN, Pleiotrophin; qRT-PCR: quantitative RT-PCR; Sh, short hairpin; Triad1, two RING fingers and DRIL 1.

markedly lower than those of rats receiving sham operation ($p < 0.001$). Besides, Triad1 overexpression increased the BBB score and incline angle of SCI rats when compared with its negative control ($p < 0.05$). Subsequently, the histomorphological changes of injured spinal cord tissues at the seventh day after surgery were examined by H&E staining and Nissl staining. In line with images from H&E staining, tissues in SCI rats exhibited severely damaged central gray matter and dorsal white matter, which were ameliorated by Triad1 overexpression (Fig. 9*C*). In Figure 9, *D* and *E*, Triad1 overexpression was observed to increase the number of ventral neurons when compared with its negative control ($p < 0.001$). These findings corroborated that Triad1 alleviated the motor function damage and histomorphological injury of SCI rats.

Discussion

SCI is an irreversible injury to nervous system, causing neurological dysfunction. How to improve the neurite outgrowth of neurons after SCI has been a hot topic in clinical and basic researches (18, 19). In this research, to explore a novel approach for SCI treatment, the SCI rat model was successfully established with motor function damage and neuron loss in spinal cord tissues. After SCI, a series of internal and external physiological and pathological changes will take place surrounding the injury site within a few hours to a few weeks (4). In this study, we uncovered that Triad1 and PTN protein expressions were upregulated in spinal cord tissues within 14 days after SCI, with the expression levels peaking on day 1 and then gradually decreasing to normal levels. Furthermore, from Co-IP assay, PTN was proved to be precipitated by Triad1. These data suggested that Triad1 and PTN might take part in the neuronal recovery after SCI, although what kinds of biological behaviors they are involved in remains unknown.

A report concerning the Triad1 regulation on neurons (20) confirmed that increased Triad1 promotes neuronal apoptosis after SCI. Another study identified that knockdown of Triad1 reduces apoptosis of spinal cord neurons (21). Triad1 contributes to the neurite outgrowth of neurons after SCI (4) and plays

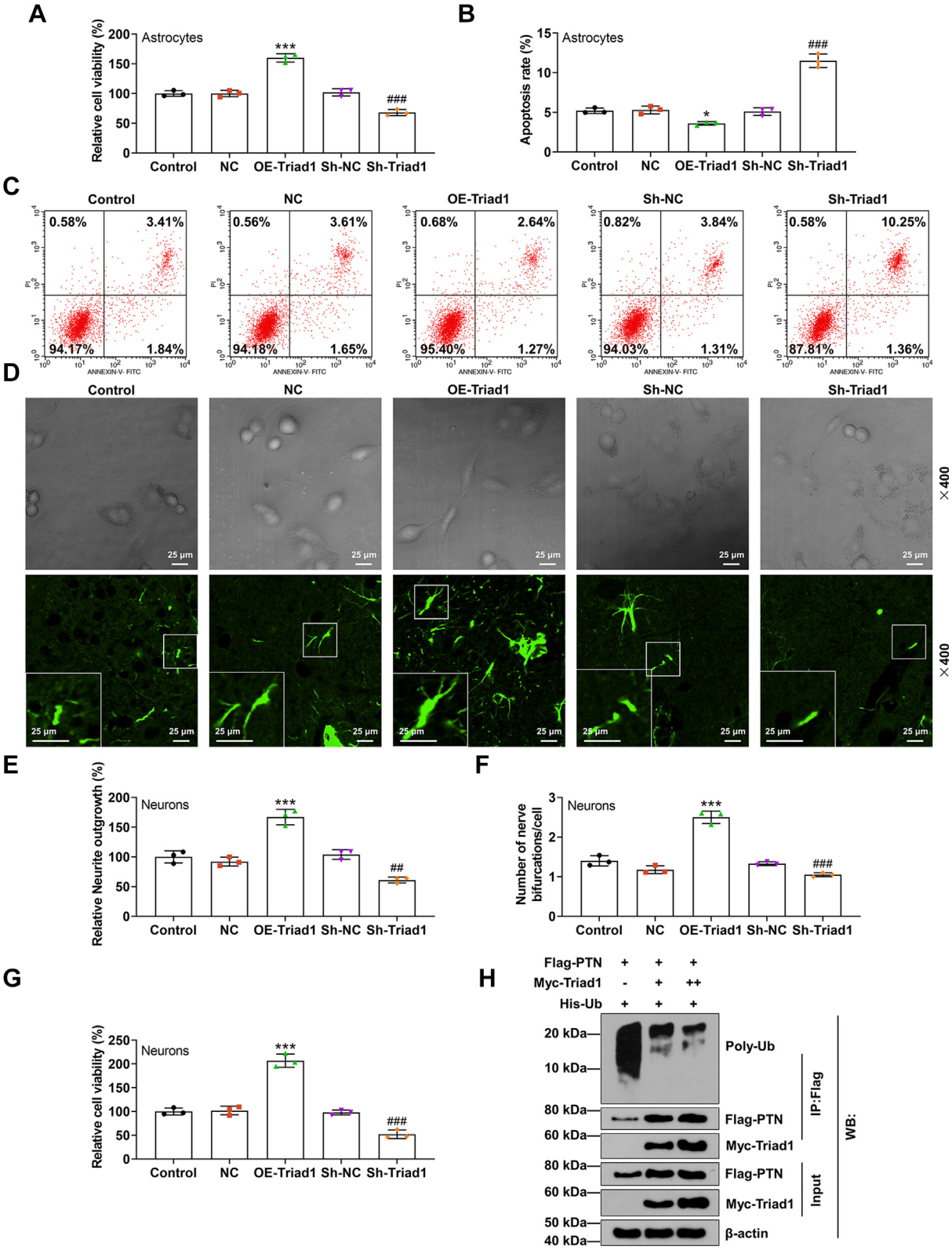

Figure 4. Triad1 overexpression promoted the viability and inhibited the apoptosis of rat astrocytes to facilitate the neurite outgrowth in rat neurons by inhibiting PTN ubiquitination. *A–C*, the viability and apoptosis of rat astrocytes after transfection were detected through MTT assay (*A*) and flow cytometry (*B* and *C*). *D–G*, after coculture of rat astrocytes with neurons, the neurite outgrowth and viability of rat neurons were detected through MAP2 immunofluorescence staining (*D–F*) and MTT assay (*G*). *H*, PTN ubiquitination in HEK-293 cells when Flag-PTN and His-ubiquitin were cotransfected with Myc-Triad1 or not was detected by Co-IP. Magnification: ×400; scale bars: 25 μm. (***$p < 0.001$, *versus* NC; $^{\#\#}p < 0.01$, $^{\#\#\#}p < 0.001$, *versus* sh-NC). Co-IP, coimmunoprecipitation; MAP2, microtubule associated protein 2; MTT, methyl thiazolyl tetrazolium; NC, negative control; OE, overexpressed; PTN, pleiotrophin; Sh, short hairpin; Triad1, two RING fingers and DRIL 1.

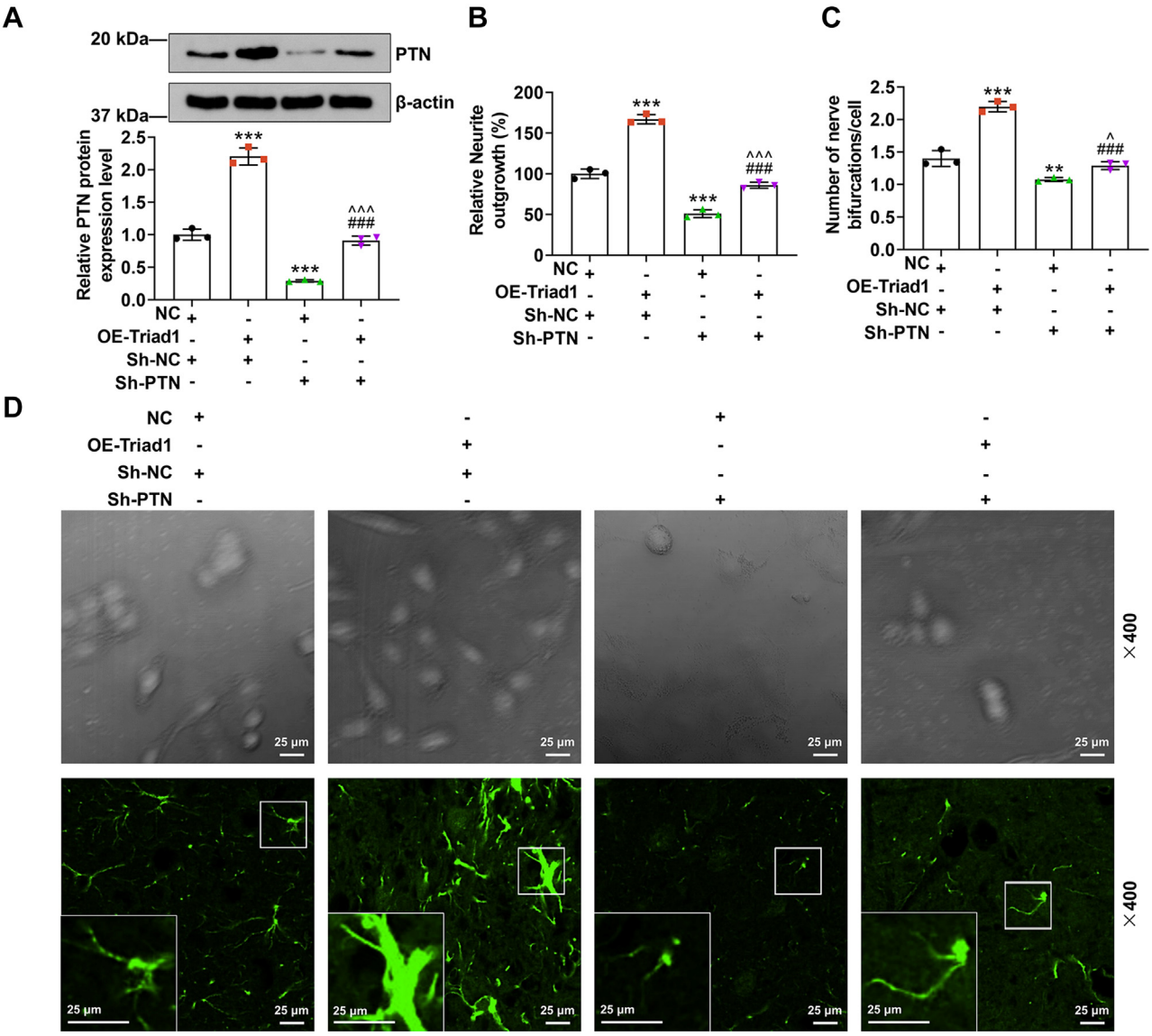

Figure 5. PTN silencing attenuated the effects of Triad1 overexpression on PTN expression in astrocytes and neurite outgrowth of rat neurons. *A*, the expression of PTN in rat astrocytes after transfection was detected through Western blot. *B–D*, after coculture of rat astrocytes with neurons, the neurite outgrowth of rat neurons was determined through MAP2 immunofluorescence staining. Magnification: ×400; scale bars: 25 μm. (**$p < 0.01$, ***$p < 0.001$, *versus* NC+sh-NC; $^{\#\#\#}p < 0.001$, *versus* OE-Triad1+sh-NC; $\hat{}p < 0.05$, $\hat{}\hat{}\hat{}p < 0.001$, *versus* NC+sh-PTN). Co-IP, coimmunoprecipitation; NC, negative control; MAP2, microtubule associated protein 2; OE, overexpressed; PTN, pleiotrophin; Sh, short hairpin; Triad1, two RING fingers and DRIL 1.

an important role in the proliferation and differentiation of neural stem cells following traumatic brain injury (8). Of note, astrocytes secrete neurotrophic factors to promote and stabilize the function of neurons in nervous system (6). Therefore, we further investigated the potential role of Triad1 in astrocytes. The similar astrocyte-specific role has also been reported by multiple scholars. For instance, Cho *et al.* demonstrated that astrocyte-dependent neurite outgrowth can be induced by valproic acid (17); and Louveau *et al.* pointed out that CD80/CD86 costimulation can direct microglia toward a repair phenotype and promote axonal outgrowth (22). Additionally, PTN was reported to reinforce microglia proliferation and secretion of neurotrophic factors to fulfill neuroprotection (16). Thus, we conjectured that the effects of Triad1 and PTN on neuron recovery were also realized through regulating astrocyte. Then, rat primary astrocytes and neurons were isolated and cultured. BDNF is a key factor affecting neuronal survival, differentiation, and plasticity, which can induce axonal outgrowth and neuronal repair (22). NGF is an important growth factor for neuronal survival (23). BDNF and NGF are secreted by astrocytes to enhance tissue repairing and neuronal rescuing (16). Of them, NGF stimulates neurite growth and neural survival after injury (24, 25), whereas BDNF promotes neuronal survival and morphogenesis (26). Sandoval-Castellanos *et al.* (27) reported that immobilizing neurotrophic factors either as NGF and BDNF or as their combination can enhance neurite outgrowth. Lee *et al.* (28) also revealed that NGF and BDNF induce neurite outgrowth *via* extracellular signal-regulated kinase (ERK) activation. Hence, increased expressions and secretion of NGF and BDNF from astrocytes may directly impact neurite outgrowth and neuronal survival as well. Data in this research uncovered that Triad1 promoted BDNF expression, NGF expression, and

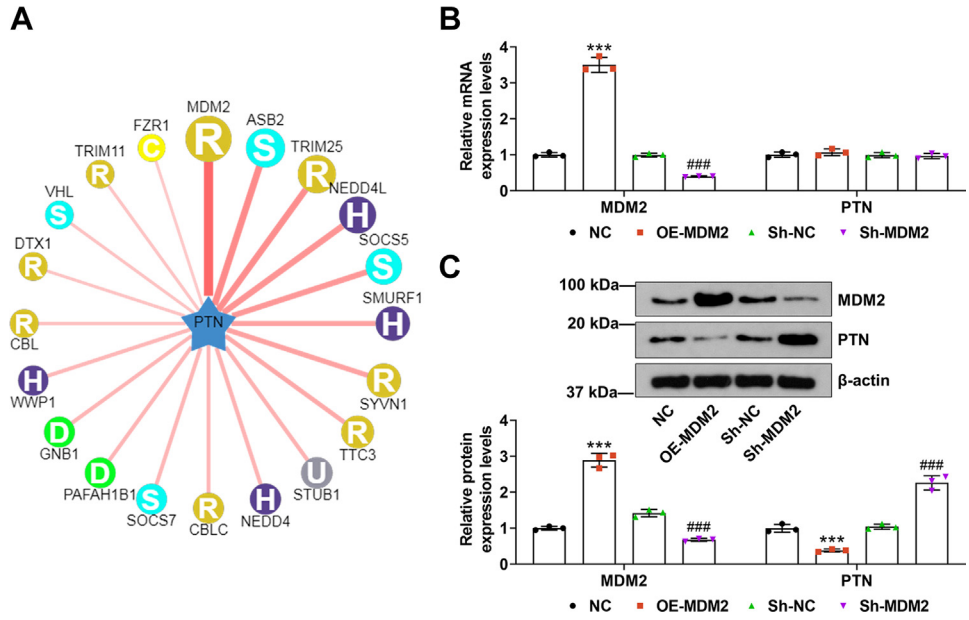

Figure 6. MDM2 overexpression downregulated the translation level of PTN while MDM2 silencing did the opposite. *A*, the factor which mediates the PTN ubiquitination was analyzed by UbiBrowser (http://ubibrowser.ncpsb.org/). *B* and *C*, after MDM2 overexpression or silencing, the transcription and translation levels of PTN were evaluated through qRT-PCR (*B*) and Western blot (*C*). (***$p < 0.001$, *versus* NC; $^{###}p < 0.001$, *versus* sh-NC). MDM2, murine double minute 2; NC, negative control; OE, overexpressed; PTN, Pleiotrophin; qRT-PCR, quantitative RT-PCR; Sh, short hairpin.

viability but blocked apoptosis in rat primary astrocytes, thereby facilitating the viability and neurite outgrowth of rat primary neurons, which indicated the promoting effect of Triad1 on neurons. PTN also stimulates the secretion of neurotrophic factors, including BDNF, ciliary neurotrophic factor (CNTF), and NGF in microglia by activating ERK 1/2 pathway (16). Thus, changes in NGF and BDNF expressions and secretion through altering PTN may be involved with ERK 1/2 pathway. Besides, consistent with data from *in vivo* assays, Triad1 upregulated PTN only in protein level and inhibited the ubiquitination of PTN. PTN is a kind of secretory neurotrophic factor that promotes microglia proliferation and secretion of neurotrophic factors to protect nerves (16, 29, 30). Similarly, in this research, PTN silencing in astrocytes dampened the neurite outgrowth of rat primary neurons and attenuated the promoting effect of Triad1 on neurite outgrowth. All these findings indicated that Triad1 promoted astrocyte-dependent neurite outgrowth by inhibiting PTN ubiquitination; however, the regulatory mechanism required in-depth exploration.

Wu *et al.* (20) demonstrated that Triad1 induces neuronal apoptosis *via* modulating the p53-caspase3 pathway following SCI. They also speculated that there may be a K63-linked polyubiquitination in the interaction between Triad1 and p53. Triad1 has been demonstrated to suppress MDM2-mediated ubiquitination and degradation of p53 through binding to p53 (13). Triad1 also modulates the neurite outgrowth of neurons following SCI (4). Upregulated Triad1 is associated with neuronal apoptosis after intracerebral hemorrhage in adult rats (31). Hence, Triad1 regulating neurons *via* the p53-caspase3 pathway may be related to MDM2-mediated ubiquitination. In this research, MDM2 was predicted as the most likely E3 ligase to regulate the PTN ubiquitination and further proved to negatively modulate PTN expression only in protein level. Although ARIH2-encoded Triad1 protein is an E3 ubiquitin ligase (32), Nutlin-3a (Mdm2 inhibitor)-induced p53 activation could be modulated by Triad1 level (33). Furthermore, the protein level of Triad1 was decreased in response to Mdm2 overexpression, which was consistent with the findings of Bae *et al.* (34). Maybe, the ubiquitin ligase activity of Triad1 is not required to regulate MDM2. Also, the present findings suggested that Triad1 antagonized MDM2-mediated PTN degradation and ubiquitination. Similarly, a previous study indicated that MDM2-induced p53 degradation can be completely suppressed by Triad1 (13). Additionally, the MDM2/p53/IGF1R axis enhances axonal sprouting and functional recovery after SCI in mice (15) and MDM2 expression is upregulated after SCI (35). Consistently, in this research, MDM2 expression was upregulated in spinal cord tissues within 14 days after SCI, in which the expression level peaked on 6 h and then gradually declined to a normal level. Besides, MDM2 diminished astrocyte, inhibited the neurite outgrowth, and further attenuated the effect of Triad1 on neurite outgrowth. These findings mirrored that Triad1 promoted astrocyte-dependent neurite outgrowth by inhibiting MDM2-mediated PTN ubiquitination.

Lastly, to verify the improving effect of Triad1 on function recovery after SCI, SCI rat model was further established. The experimental data reflected that Triad1 ameliorated the motor function damage and neuron loss of SCI rats, which further confirmed that Triad1 promoted astrocyte-dependent neurite outgrowth and function recovery after SCI by inhibiting MDM2-mediated PTN ubiquitination.

In conclusion, our research authenticates that Triad1 inhibits MDM2-mediated PTN ubiquitination to promote astrocyte-dependent neurite outgrowth, thereby improving recovery after SCI, which contributes to a novel theoretical basis for SCI research and treatment.

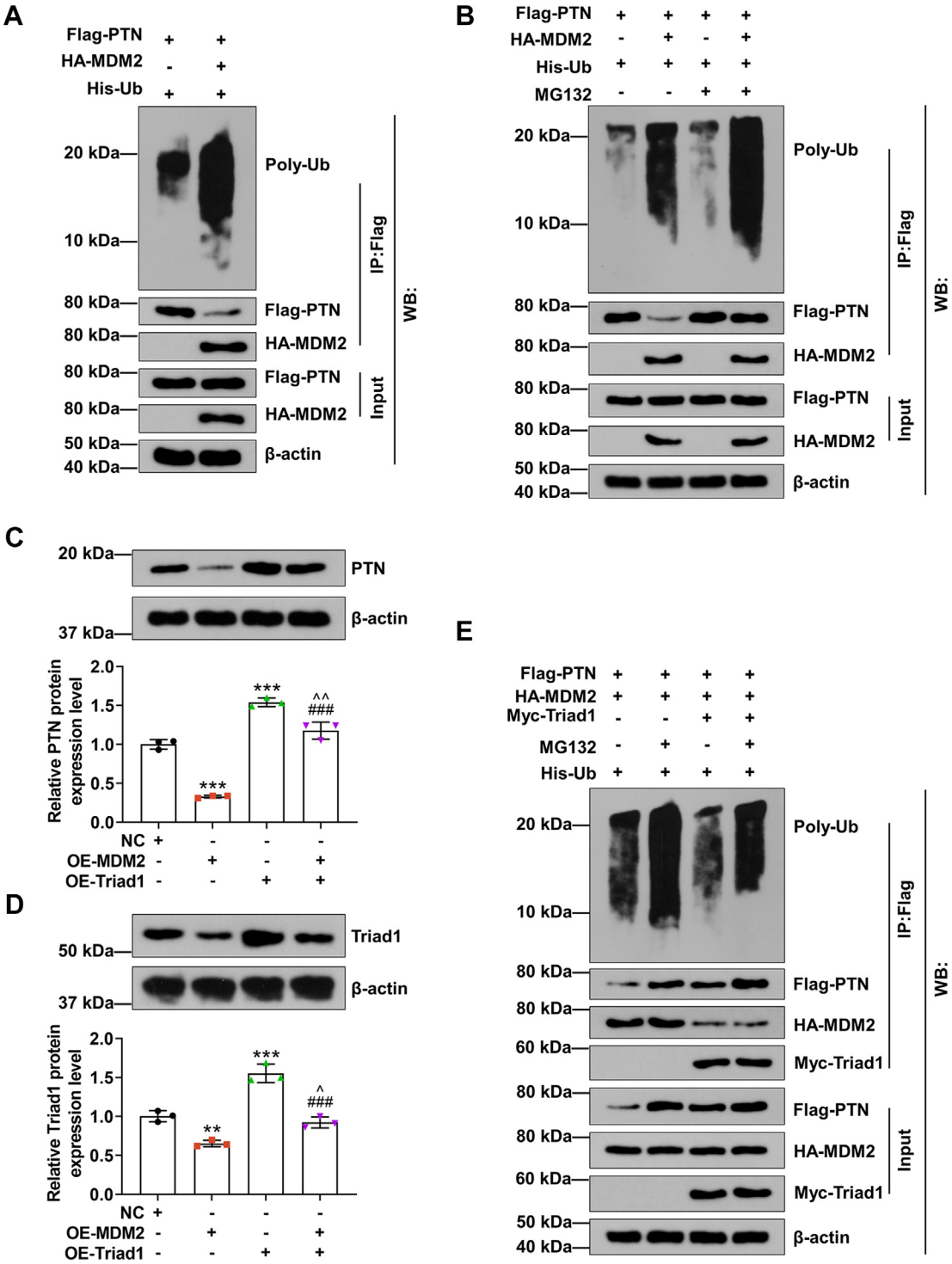

Figure 7. Triad1 inhibited the MDM2-mediated PTN ubiquitination in HEK-293 cells. *A*, PTN ubiquitination in HEK-293 cells when Flag-PTN and His-ubiquitin were cotransfected with HA-MDM2 or not was detected by Co-IP. *B*, in the presence or absence of MG132, PTN ubiquitination in HEK-293 cells when Flag-PTN and His-ubiquitin were cotransfected with HA-MDM2 or not was determined by Co-IP. *C* and *D*, the protein expressions of PTN and Triad1 in astrocytes transfected with plasmids overexpressing MDM2 and Triad1 were detected by Western blot. *E*, in the presence or absence of MG132, PTN ubiquitination in HEK-293 cells when Flag-PTN, His-ubiquitin, and HA-MDM2 were cotransfected with Myc-Triad1 or not was detected by Co-IP. (***$p < 0.001$, *versus* NC; $^{\#\#\#}p < 0.001$, *versus* OE-MDM2; $^{\wedge\wedge}p < 0.01$, *versus* OE-Triad1). Co-IP, coimmunoprecipitation; MDM2, murine double minute 2; NC, negative control; OE, overexpressed; PTN, pleiotrophin; Triad1, two RING fingers and DRIL 1.

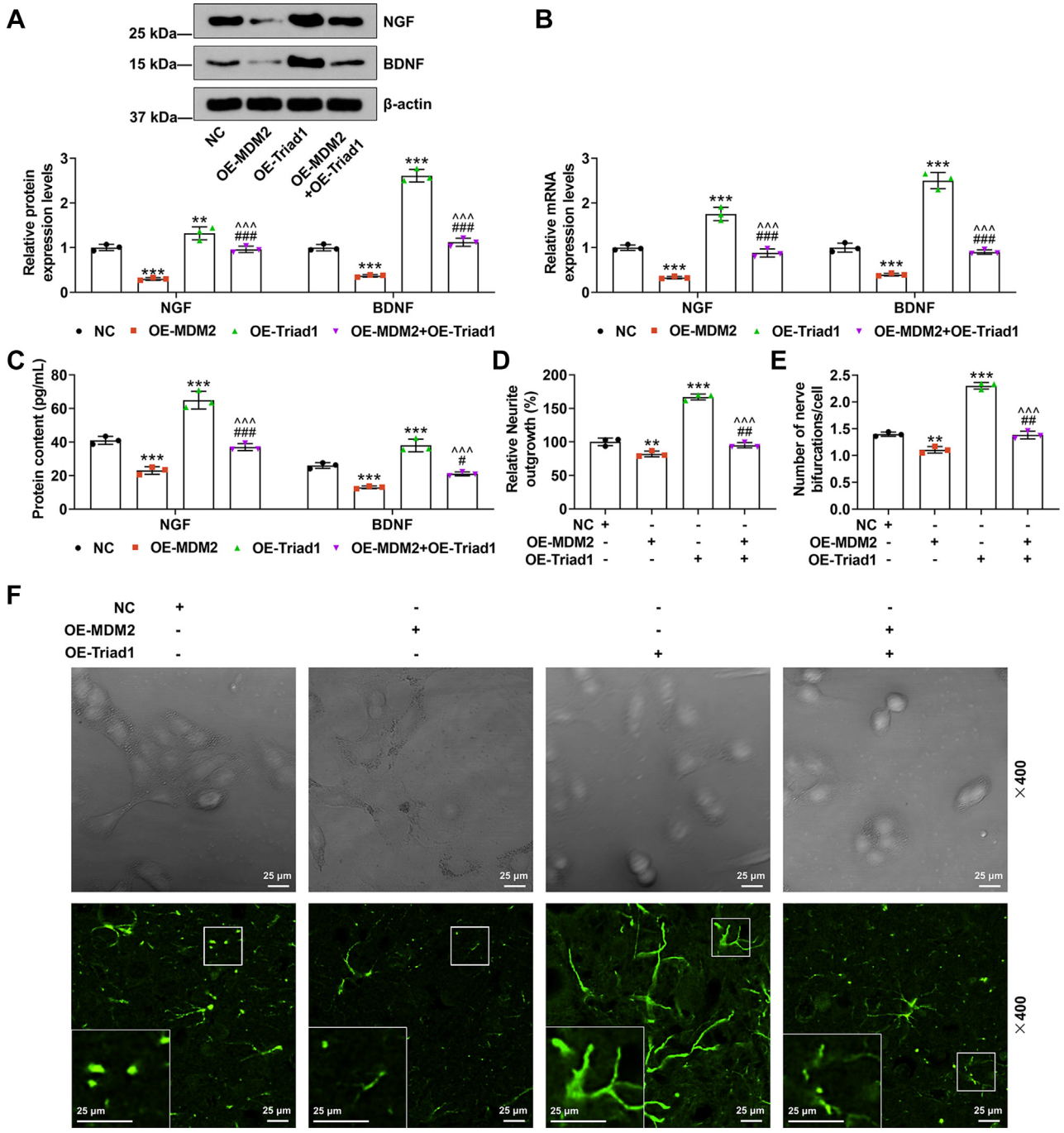

Figure 8. MDM2 attenuated the promoting effect of Triad1 up-regulation on NGF and BDNF expressions in rat astrocytes and neurite outgrowth of rat neurons. *A* and *B*, the transcription and translation levels of NGF and BDNF in astrocytes after transfection were evaluated by Western blot (*A*) and qRT-PCR (*B*). *C*, the secretion of NGF and BDNF in culture supernatant of astrocytes was assessed by ELISA. *D–F*, after coculture of rat astrocytes with neurons, the neurite outgrowth of rat neurons was detected through MAP2 immunofluorescence staining. Magnification: ×400; scale bars: 25 μm. (**$p < 0.01$, ***$p < 0.001$, *versus* NC; $^{\#}p < 0.05$, $^{\#\#}p < 0.01$, $^{\#\#\#}p < 0.001$, *versus* OE-MDM2; $\widetilde{}\widetilde{}p < 0.01$, *versus* OE-Triad1). BDNF, brain-derived neurotrophic factor; MAP2, microtubule associated protein 2; MDM2, murine double minute 2; NC: negative control; NGF, nerve growth factor; OE, overexpressed; qRT-PCR, quantitative RT-PCR; Triad1, two RING fingers and DRIL 1.

Experimental procedures

Animals and ethics statement

All Sprague–Dawley rats were obtained from Nantong University and fed in the specific pathogen-free condition with 12 h of light/dark cycle and a free diet. Before experiments, all animals received adaptive feed for 5 days. The animal experiments were approved by the Committee of Experimental Animals of Nantong University (No. 20170222-001). Efforts were made to minimize pain of the animals. All procedure and experiments were performed at Nantong University.

Primary astrocyte culture

Rat astrocytes were isolated from the frontal cortices of 1 to 2 day old Sprague–Dawley rat pups according to the previous research (17). In brief, the frontal cortices of rats were harvested

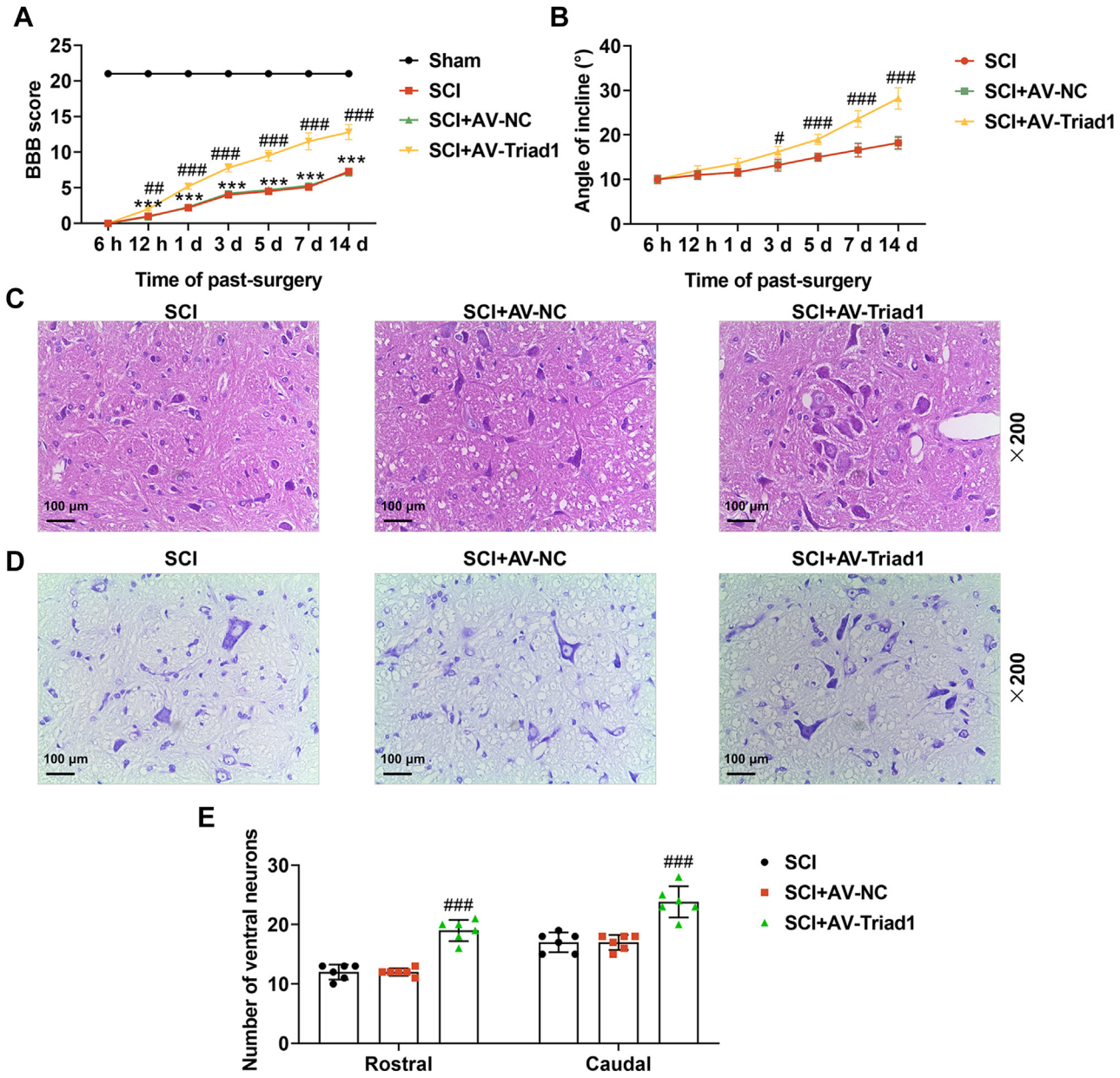

Figure 9. Triad1 alleviated the motor function damage and histomorphological injury of SCI rats. *A* and *B*, after SCI rat model was pretreated with Triad1 overexpression adenovirus, the motor function of all rats was evaluated through BBB locomotion rating scale (*A*) and the inclined plane test (*B*). *C–E*, the histomorphological changes of injured spinal cord tissues at 7 days after surgery were then examined by H&E staining (*C*) and Nissl staining (*D*), and the number of ventral neurons was calculated (*E*). Magnification: ×200; scale bars: 100 μm. (***$p < 0.001$, *versus* sham; $^{\#}p < 0.05$, $^{\#\#}p < 0.01$, $^{\#\#\#}p < 0.001$, *versus* SCI+AV-NC). AV, adenovirus; BBB, Basso, Beattie, and Bresnahan; NC, negative control; SCI, spinal cord injury; Triad1, two RING fingers and DRIL 1.

and digested with trypsin (25200072, Gibco) to obtain cells. Then, the cells were seeded onto poly-d-lysine–coated plates (152035, Thermo Scientific) and cultured with Dulbecco's modified Eagle's medium (DMEM)/F12 medium (11330032, Gibco) containing 10% fetal bovine serum (10099141, Gibco). Thereafter, the cells were collected and incubated in a new 6-well plate (714011, Nest) with DMEM/F12 medium containing 10% fetal bovine serum at 37 °C in a humidified environment with 5% CO_2. Astrocytes aged 13 to 14 days were used in this research.

Primary cortical neuron culture

Rat cortical neurons were isolated from Sprague-Dawley rats at the embryonic day 18 as a previous research reported (17). Briefly, the cortical region without meninges was mechanically dissociated in neuronal culture medium (88283, Thermo Scientific). Then the cells were collected, seeded onto poly-d-lysine–coated plate and cultured in neuronal culture medium at 37 °C in a humidified environment with 5% CO_2.

Astrocyte transfection

Prior to transfection, plasmids overexpressing Triad1 and MDM2, their negative control (NC), shRNAs targeting Triad1 (sh-Triad1), PTN (sh-PTN) and MDM2 (sh-MDM2), and NC of shRNA (sh-NC) were synthesized in RIBOBIO. For transfection, astrocytes were cultured in a 6-well plate until 90% confluence was reached. Then, the aforementioned plasmids

and shRNAs were separately transfected into the cells with the help of Lipofectamine 2000 CD transfection reagent (12566014, Invitrogen). After 48 h of transfection, the cells were collected for later use.

Coculture of neuron with astrocyte

A major advantage of the coculture system over neurons alone is to support the growth, survival, and differentiation of nutrient factors secreted by the glial feeding layer, which more accurately resembles the environment *in vivo*; moreover, the coculture can be applied to explore neuronal-glial interactions (36). The coculture of neuron with astrocyte was performed as previously illuminated (17, 37). Before coculture, transfected or untransfected astrocytes were cultured in 24-well plates. Meanwhile, neurons (1×10^4 cells/coverslip) were plated in glass coverslips to which 3 to 4 beads of paraffin (A13912, OKA) were previously affixed. After 30 min (min) of incubation in neuronal culture medium to allow for neurons to attach, the glass coverslips were inverted in a 24-well plate above the astrocyte monolayer (the paraffin drops to prevent neuron-astrocyte contact) for coculture for 3 days. After that, the glass coverslips were taken out from the 24-well plate and the neurons on the glass coverslips were firstly observed under a DMi8 S optical microscope (Leica) at 400× magnification. Then, the growth and viability of neurons were detected by microtubule-associated protein 2 (MAP2) immunofluorescence staining and methyl thiazolyl tetrazolium (MTT) assay, respectively.

Immunofluorescence staining

The immunofluorescence staining was conducted as previously illustrated (38). After coculture with astrocytes, the neurons were fixed by 4% paraformaldehyde (P0099, Beyotime) for 20 min. Then, the samples were further incubated with a solution containing 10% goat serum (16210072, Gibco), 3% bovine serum albumin (P0007, Beyotime), and 0.1% Triton X-100 (ST797, Beyotime) for 30 min, followed by the incubation with anti-MAP2 antibody (#8707, CST) at 4 °C overnight. On the next day, the samples were further cultured with goat anti-rabbit IgG Alexa Fluor 488 (ab150077, AbcamUK) for 1 h. Finally, the samples were observed using a DM2500 fluorescence microscope (Leica) under 400× magnification.

The identification of neurons or astrocytes was achieved *via* neuron-specific nuclear protein (NeuN) or astrocyte marker (GFAP) immunofluorescent labeling (39). Anti-NeuN antibody (AF1072, Beyotime, 1:200) or GFAP rabbit mAb (AF1177, Beyotime, 1:200) was used. The rabbit serum control group was set up in parallel. Neurons or astrocytes were incubated with the primary antibody and then rinsed with PBS (C0221A, Beyotime). Neurons or astrocytes in coverslips were probed for 1 h with an Alexa Fluor 488 goat anti-rabbit IgG (A0423, Beyotime, 1:500) at 37 °C, after which 4′,6-diamidino-2-phenylindole (C0060, Solarbio, 1:100) was used to counterstain these cells. Ultimately, cells were evaluated *via* fluorescence microscopy.

MTT assay

The viability of neurons and astrocytes after treatment was determined using MTT assay. In a nutshell, the cells with different treatments in a 96-well plate were incubated with 0.5 mg/ml MTT buffer (ST316, Beyotime) for 4 h. Then, after the MTT buffer was absorbed, 100 μl dimethyl sulfoxide (ST038, Beyotime) was further added into each well. After the formazan in cells was fully dissolved, the cell viability in each well was detected by a Varioskan LUX microplate reader (Thermo Scientific) under 572 nm wavelength.

Flow cytometry

The apoptosis of astrocytes after transfection was assessed using an Annexin V-FITC cell apoptosis detection kit (C1062S, Beyotime) by flow cytometry. To be specific, the transfected astrocytes were collected and washed with PBS (C0221A, Beyotime) three times. Then, the astrocytes were suspended with 195 μl Annexin V-FITC binding buffer, followed by the addition of 5 μl Annexin V-FITC and 10 μl propidium iodide. After the astrocytes were incubated for 20 min in the dark, the cell apoptosis signal was detected by a flow cytometer (Attune NxT; Thermo Scientific).

ELISA

Expressions of NGF and BDNF in culture supernatant of astrocytes were quantitated using ELISA. The detection kits of NGF (MM-0187R2) and BDNF (MM-0209R1) were bought from MEIMIAN. Specifically, the culture supernatant was added into a specific 96-well plate and reacted at 37 °C for 30 min. Then, the plate was washed with washing buffer five times, after which the enzyme reagent was added for reaction at 37 °C for 30 min. Subsequently, chromogenic buffer A and B were added to react with cells at 37 °C for 10 min. Finally, the reaction was terminated by stopping buffer, and the absorbance of each well was read by a Varioskan LUX microplate reader.

Quantitative RT-PCR

The expressions of related genes in astrocytes were analyzed using quantitative RT-PCR. In detail, the transfected astrocytes were collected and treated with TRIeasy LS Total RNA Extraction Reagent (19201ES60, YEASEN). Then, the extracted RNA was reverse transcribed into complementary DNA (cDNA) using the Hifair II 1st Strand cDNA Synthesis Kit (11119ES60, YEASEN). Afterward, 1 μl cDNA, 2 μl gene primers, 10 μl Hieff UNICON Universal Blue qPCR SYBR Green Master Mix (11184ES03, YEASEN), and 7 μl DEPC-treated Water (10601ES76, YEASEN) were mixed and the PCR was performed under 7500 Fast Instrument (Applied Biosystems). The condition of reaction was set as follows: predenaturation at 95 °C for 2 min, denaturation at 95 °C for 10 s (s), and annealing/extension at 60 °C for 20 s with 40 cycles from denaturation to annealing/extension. Finally, the gene relative expression level was calculated using $2^{-\triangle\triangle CT}$ method with the 7500 Fast Instrument. β-actin was applied as

the internal control. All primers in this experiment are shown in Table 1.

Establishment of a SCI rat model

Male Sprague-Dawley rats (200–250 g) were used to construct the SCI rat model in this experiment according to the previous research (40). The rats were anesthetized with 5% isoflurane (R51022, RWD) to implement surgery. Subsequently, the T9-T10 lamina and spinous process of all rats were excised to expose the spinal cord. The SCI model was constructed by striking the T9 segment of spinal cord with a 10 g hammer from a height of 25 mm. The incision was sutured layer by layer. Rats in the sham group only underwent laminectomy without severe blow operation. After surgery, all rats were fed normally and observed closely.

Animal experimental protocol

Animal experiments contained two parts.

In terms of the first part (total 52 rats involved), the rats were divided into sham group (n = 10) and SCI group (n = 42). Rats in SCI group received SCI surgery while those in sham group only underwent laminectomy without severe blow operation. After surgery, all rats were fed normally and observed closely. BBB locomotion rating scale (41) and the inclined plane test were performed at 6 h and 12 h, 1st day, 3rd day, 5th day, 7th day, and 14th day after surgery to evaluate the locomotion recovery. In addition, for rats in SCI group, after locomotion recovery evaluation at 6 h and 12 h, 1st day, 3rd day, 5th day, and 7th day, spinal cord tissues containing the spinal cord lesion (1 cm on each side of the lesion) from six rats were harvested for further experiments, while those from the remaining rats who were sacrificed in the two groups were collected after locomotion recovery evaluation at the 14th day.

For the second part (total 46 rats involved), the rats were assigned into four groups: sham group (n = 10), SCI group (n = 12), SCI+AV-NC group (n = 12), and SCI+AV-Triad1 group (n = 12). Rats in SCI group received SCI surgery while those in sham group only underwent laminectomy without severe blow operation. Rats in SCI+AV-NC and SCI+AV-Triad1 groups were intrathecally preinjected with the adenoviruses with NC (AV-NC) and adenoviruses with Triad1 overexpression plasmid (AV-Triad1) at 2 days before SCI surgery in accordance with a previous report (42). Motor function of rats in SCI+AV-NC and SCI+AV-Triad1 groups after intrathecal injection was all unaffected. After surgery, all rats were fed normally and observed closely. BBB locomotion rating scale and the inclined plane test were carried out at 6 h and 12 h, 1st day, 3th day, 5th day, 7th day, and 14th day after surgery to evaluate the locomotion recovery. In addition, after locomotion recovery evaluation at the seventh day, spinal cord tissues containing the spinal cord lesion (1 cm on each side of the lesion) from six rats in each group were collected for the H&E staining and Nissl staining.

Locomotion recovery evaluation

The locomotion function of rats after surgery was evaluated by BBB locomotion rating scale and the inclined plane test as per the previous publication (43). In brief, the BBB score ranged from 0 to 21, with 0 for unobservable movement and 21 for normal movement. For the inclined plane test, the free edge of the plate was gradually raised to increase the angle of inclination. The maximum angle at which the rats were kept stable for at least 5 s was recorded as the test angle. All results in the two experiments were evaluated by three independent reviewers who were unaware of the experimental conditions.

H&E staining

The H&E staining kit (C0105S) was firstly purchased from Beyotime. The obtained spinal cord tissues were fixed with 4% paraformaldehyde, embedded in paraffin, and cut into 5 μm slices. Then, the slices were dewaxed by xylene (X821391, Macklin), incubated with 100% ethanol (E809056, Macklin) for 5 min, 90% ethanol for 2 min, 80% ethanol for 2 min, and 70% ethanol for 2 min, and washed by distilled water for 2 min in turn. After that, hematoxylin was used to stain the slices for 10 min followed by washing with distilled water. After being colored with eosin for 1 min, the slices were further incubated with 70% ethanol (10 s), 80% ethanol (10 s), 90% ethanol (10 s), 100% ethanol (10 s), and xylene (5 min). Finally, the slices were added with neutral gum (D11029, OKA) and observed under THUNDER imaging system (Leica) at 200× magnification.

Nissl staining

The collected spinal cord tissues were also fixed with 4% paraformaldehyde, embedded in paraffin, and cut into 5 μm slices. Then, the slices were dewaxed by xylene, incubated with 100% ethanol (5 min), 90% ethanol (2 min), 80% ethanol (2 min), and 70% ethanol (2 min), and washed by distilled water for 2 min in turn. Thereafter, the slices were cultured with 1% toluidine blue buffer (BB-44526-1, BestBio) at 54 °C for 25 min. After being washed with distilled water for 3 min, the slices were further cultivated with 70% ethanol (10 s), 80% ethanol (10 s), 90% ethanol (10 s), 100% ethanol (10 s), and xylene (5 min). Ultimately, the slices were added with neutral gum and observed under THUNDER imaging system at 200×

Table 1
All qRT-PCR primers in this study

Target gene	Forward primers, 5′-3′	Reverse primers, 5′-3′
Triad1	CGGGTACAGGAGCCTAGAGCTCGCCG	GGATTGTGGCACAGTCTGTGGGTGCG
PTN	GAAAATTTGCAGCTGCCTTC	CACACACTCCATTGCCATTC
MDM2	GCCTGGATCAGGATTCAGTTTCTG	GTGACCCGATAGACCTCATCATCC
NGF	TGCATAGCGTAATGTCCATGTTG	CTGTGTCAAGGGAATGCTGAA
BDNF	CAAAAGGCCAACTGAAGC	CGCCAGCCAATTCTCTTT
β-actin	CCCGCGGAGTACAACCTTCT	CGTCATCCATGGCGAACT

magnification. Correspondingly, the number of ventral neurons at 5 mm from the rostral and 5 mm from the caudal was counted.

Immunohistochemistry assay

Spinal cord tissues were collected and fixed with 4% paraformaldehyde. After the sample was embedded in paraffin and cut into 5 μm slices, the slices were dewaxed by xylene, cultured with 100% ethanol (5 min), 90% ethanol (2 min), 80% ethanol (2 min), and 70% ethanol (2 min), and washed by distilled water for 2 min in turn. Then, the slices were repaired by antigen retrieval solution (P0088, Beyotime) and separately incubated with primary antibodies, including anti-Triad1 antibody (PA5-70369, 1:100, Invitrogen), anti-MDM2 antibody (PA5-86249, 1:200, Invitrogen), and anti-PTN antibody (PA5-94984, 1:200, Invitrogen) at 4 °C overnight. Then, the slices were incubated with the secondary antibody goat anti-rabbit antibody (ab6721, 1:1000, Abcam) for 2 h. Subsequently, the slices were treated using the ABC detection immunochemistry kit (ab64261, Abcam) and stained with hematoxylin (M18300, Meryer). After washing with distilled water for 3 min, the slices were incubated with 70% ethanol (10 s), 80% ethanol (10 s), 90% ethanol (10 s), 100% ethanol (10 s), and xylene (5 min). Finally, the slices were added with neutral gum and observed under THUNDER imaging system at 200× magnification.

Double immunofluorescence staining

Spinal cord tissues were prepared similar to the procedure in the immunohistochemistry assay. The samples were blocked using 5% bovine serum albumin in PBS and then incubated with antibodies. The reagents used were anti-Triad1 (rabbit, ab208624), anti-PTN (mouse, sc-74443, 1:50, Santa Cruz Biotechnology (SCBT)) and anti-MDM2 (mouse, 1:1000, ab216076, Abcam) antibodies or different cell markers including NeuN (neuron marker, mouse, GTX30773, 1:100; SCBT), GFAP (astrocytes marker, mouse, ab4648, 1:100; Abcam)), and goat antimouse IgG H&L (Alexa Fluor 488) (ab150113, 1:1000; Abcam) secondary antibody. The immunofluorescence was assessed under a fluorescence microscopy (20). The intensity was analyzed with ImageJ, and the relative fluorescence intensity was calculated through dividing the red fluorescence intensity by the green fluorescence intensity and finally normalized this value to the sham group.

Western Blot assay

Total proteins in cultured astrocytes and tissues collected form rats were firstly isolated using NP-40 lysis solution (KGP705, KeyGEN BioTECH) followed by centrifugation (14,000*g*) at 4 °C for 30 min. The concentration of the proteins was measured using a microplate reader with the help of a BCA Detection Kit (P0011, Beyotime). Then, the proteins were denatured by mixing with loading buffer (M52282, MERYER) and heating at 100 °C for 5 min. After that, the proteins were separated by the SDS-PAGE gel (P0012A, Beyotime) and further transferred onto polyvinylidene difluoride membrane (FFP24, Beyotime). The polyvinylidene difluoride membrane was then incubated with Western blot blocking buffer (KGP108, KeyGEN BioTECH) for 2 h, related primary antibodies at 4 °C for 16 h, and secondary antibodies for 2 h on the next day. Finally, the protein band in the membrane was detected by an Image Lab 3.0 detector (Bio-Rad) with the help of Super ECL Plus Super Sensitive Luminescent Liquid (M41129, MERYER). Primary antibodies used were those against MDM2 (1:1000, ab259265, 90 kDa, Abcam), PTN (1:1000, ABIN3181062, 19 kDa, Antibodies), Triad1 (1:3000, ab133653, 57 kDa, Abcam), NGF (1:500, ab52918, 27 kDa, Abcam), BDNF (1:6000, ab108319, 15 kDa, Abcam), and β-actin (1:10,000, 42 kDa, ab8226, Abcam). Secondary antibodies included goat-anti-rabbit IgG (1:20,000, ab6721, Abcam) and goat antimouse IgG (1:10,000, ab6789, Abcam).

Co-IP analysis

For Co-IP analysis using rat tissues, total proteins in tissues were firstly isolated utilizing immunoprecipitation lysis buffer (P0013, Beyotime) and then incubated with Triad1- or PTN-conjugated protein beads (10006D, Invitrogen) according to the instructions. After the beads were eluted, the precipitation of protein complex was examined through Western blot. The Co-IP analysis was performed using HEK-293 cells or astrocytes referring to the previous research (44). HEK-293 cells were obtained from Procell (CL-0001) and cultured in HEK-293 specific medium (CM-0001, Procell) at 37 °C in a humidified environment with 5% CO_2. Before experiments, HEK-293 cells and astrocytes were transfected with Flag-PTN, Myc-Triad1, His-Ub, and HA-MDM2 and isolated using immunoprecipitation lysis buffer. Then, the proteins were incubated with anti-Flag Magnetic Beads (P2115, Beyotime) at 4 °C overnight. After the beads were eluted, the precipitation of protein complex was examined through Western blot. Antibodies against Ub Polyclonal (abs146503, 1:1000, Absin), Flag (#14793, 1:50, CST), Myc (#2276, 1:1000, CST), and HA (#3724, 1:50, CST) were used.

Statistical analysis

All analyses in this research were performed with the help of GraphPad prism 8.0 (GraphPad Software Inc). Independent samples *t* test was used to analyze data from two groups. One-way ANOVA with Bonferroni post hoc test was applied to analyze data from multiple groups. $p < 0.05$ was considered statistically significant. Statistical data were described as mean ± SD.

Data availability

The analyzed datasets generated during the study are available from the corresponding author on reasonable request.

Supporting information—This article contains supporting information.

Acknowledgments—This work was supported by the National Natural Science Foundation of China[81771319]; the Medical Scientific Research Project of Jiangsu Provincial Health Commission [ZDB2020004]; the Six Talent Peak Funding Projects in Jiangsu Province[2017-WSW-156]; the Scientific Research Project of Nantong Municipal Health Commission[MA2021016]; the Youth Fund of National Natural Science Foundation of China [82002394]; the Jiangsu Young Medical Talents Funding Project [QNRC2016413]; the Nantong Social Livelihood Science and Technology Project[MS12019027]; the Jiangsu Graduate Research and Practice Innovation Program[KYCX21_3107]; the Nantong Science and Technology Project[JC2020013].

Author contributions—C. W. conceptualization; C. W. methodology; G. X., G. B., H. G., J. C., J. Z., C. C., H. H., P. X., J. J., Y. L., J. H., Y. S., J. F., Y. L., and Z. C. formal analysis; C. W., G. X., G. B., H. G., J. C., J. Z., C. C., H. H., P. X., J. J., Y. L., J. H., Y. S., J. F., Y. L., and Z. C. writing–review & editing; C. W., G. X., G. B., H. G., J. C., J. Z., C. C., H. H., P. X., J. J., Y. L., J. H., Y. S., J. F., Y. L., and Z. C. supervision.

Conflict of interest—The authors declare that they have no conflicts of interest with the contents of this article.

Abbreviations—The abbreviations used are: BBB, Basso, Beattie, and Bresnahan; BDNF, brain-derived neurotrophic factor; cDNA, complementary DNA; Co-IP, coimmunoprecipitation; NC, negative control; NGF, nerve growth factor; PTN, pleiotrophin; SCI, spinal cord injury.

References

1. Ashammakhi, N., Kim, H. J., Ehsanipour, A., Bierman, R. D., Kaarela, O., Xue, C., *et al.* (2019) Regenerative therapies for spinal cord injury. *Tissue Eng. Part B Rev.* **25**, 471–491
2. Holmes, D. (2017) Spinal-cord injury: spurring regrowth. *Nature* **552**, S49
3. Kwon, B. K., Bloom, O., Wanner, I. B., Curt, A., Schwab, J. M., Fawcett, J., *et al.* (2019) Neurochemical biomarkers in spinal cord injury. *Spinal Cord* **57**, 819–831
4. Wu, C., Bao, G., Xu, G., Sun, Y., Wang, L., Chen, J., *et al.* (2019) Triad1 regulates the expression and distribution of EHD1 contributing to the neurite outgrowth of neurons after spinal cord injury. *J. Cell Biochem.* **120**, 5355–5366
5. Fan, B., Wei, Z., Yao, X., Shi, G., Cheng, X., Zhou, X., *et al.* (2018) Microenvironment imbalance of spinal cord injury. *Cell Transpl.* **27**, 853–866
6. Kroner, A., and Rosas Almanza, J. (2019) Role of microglia in spinal cord injury. *Neurosci. Lett.* **709**, 134370
7. Cotton, T. R., and Lechtenberg, B. C. (2020) Chain reactions: molecular mechanisms of RBR ubiquitin ligases. *Biochem. Soc. Trans.* **48**, 1737–1750
8. Jiang, R., Liu, Q., Zhu, H., Dai, Y., Yao, J., Liu, Y., *et al.* (2018) The expression of TRIAD1 and DISC1 after traumatic brain injury and its influence on NSCs. *Stem Cell Res. Ther.* **9**, 297
9. Hassink, G., Slotman, J., Oorschot, V., Van Der Reijden, B. A., Monteferrario, D., Noordermeer, S. M., *et al.* (2012) Identification of the ubiquitin ligase Triad1 as a regulator of endosomal transport. *Biol. Open* **1**, 607–614
10. Nakamura, N. (2018) Ubiquitin system. *Int. J. Mol. Sci.* **19**, 1080
11. Faktor, J., Pjechova, M., Hernychova, L., and Vojtesek, B. (2019) Protein ubiquitination research in oncology. *Klin. Onkol.* **32**, 56–64
12. Popovic, D., Vucic, D., and Dikic, I. (2014) Ubiquitination in disease pathogenesis and treatment. *Nat. Med.* **20**, 1242–1253
13. Bae, S., Jung, J. H., Kim, K., An, I. S., Kim, S. Y., Lee, J. H., *et al.* (2012) TRIAD1 inhibits MDM2-mediated p53 ubiquitination and degradation. *FEBS Lett.* **586**, 3057–3063
14. Buetow, L., and Huang, D. T. (2016) Structural insights into the catalysis and regulation of E3 ubiquitin ligases. *Nat. Rev. Mol. Cell Biol.* **17**, 626–642
15. Joshi, Y., Soria, M. G., Quadrato, G., Inak, G., Zhou, L., Hervera, A., *et al.* (2015) The MDM4/MDM2-p53-IGF1 axis controls axonal regeneration, sprouting and functional recovery after CNS injury. *Brain* **138**, 1843–1862
16. Miao, J., Ding, M., Zhang, A., Xiao, Z., Qi, W., Luo, N., *et al.* (2012) Pleiotrophin promotes microglia proliferation and secretion of neurotrophic factors by activating extracellular signal-regulated kinase 1/2 pathway. *Neurosci. Res.* **74**, 269–276
17. Cho, K. S., Kwon, K. J., Choi, C. S., Jeon, S. J., Kim, K. C., Park, J. H., *et al.* (2013) Valproic acid induces astrocyte-dependent neurite outgrowth from cultured rat primary cortical neuron *via* modulation of tPA/PAI-1 activity. *Glia* **61**, 694–709
18. Eckert, M. J., and Martin, M. J. (2017) Trauma: spinal cord injury. *Surg. Clin. North Am.* **97**, 1031–1045
19. Carter, G. T. (2014) Spinal cord injury rehabilitation. *Phys. Med. Rehabil. Clin. N. Am.* **25**, xiii–xiv
20. Wu, C., Zhang, H., Hong, H., Chen, C., Chen, J., Zhang, J., *et al.* (2022) E3 ubiquitin ligase Triad1 promotes neuronal apoptosis by regulating the p53-caspase3 pathway after spinal cord injury. *Somatosensory Mot. Res.* **39**, 21–28
21. Shen, X., Zhang, Y., Zhu, H., Sun, Y., Wang, W., Zhou, Z., *et al.* (2022) Triad1 promotes the inflammatory response and neuronal apoptosis to aggravate acute spinal cord injury in rats. *Comput. Math. Met. Med.* **2022**, 2025756
22. Louveau, A., Nerriere-Daguin, V., Vanhove, B., Naveilhan, P., Neunlist, M., Nicot, A., *et al.* (2015) Targeting the CD80/CD86 costimulatory pathway with CTLA4-Ig directs microglia toward a repair phenotype and promotes axonal outgrowth. *Glia* **63**, 2298–2312
23. Allen, S. J., Watson, J. J., Shoemark, D. K., Barua, N. U., and Patel, N. K. (2013) GDNF, NGF and BDNF as therapeutic options for neurodegeneration. *Pharmacol. Ther.* **138**, 155–175
24. Hu, J., Tian, L., Prabhakaran, M. P., Ding, X., and Ramakrishna, S. (2016) Fabrication of nerve growth factor encapsulated aligned poly(ε-Caprolactone) nanofibers and their assessment as a potential neural tissue engineering scaffold. *Polymers* **8**, 54
25. Zhao, Y. Z., Jiang, X., Xiao, J., Lin, Q., Yu, W. Z., Tian, F. R., *et al.* (2016) Using NGF heparin-poloxamer thermosensitive hydrogels to enhance the nerve regeneration for spinal cord injury. *Acta Biomater.* **29**, 71–80
26. Numakawa, T., Suzuki, S., Kumamaru, E., Adachi, N., Richards, M., and Kunugi, H. (2010) BDNF function and intracellular signaling in neurons. *Histol. Histopathol.* **25**, 237–258
27. Sandoval-Castellanos, A. M., Claeyssens, F., and Haycock, J. W. (2020) Biomimetic surface delivery of NGF and BDNF to enhance neurite outgrowth. *Biotechnol. Bioeng.* **117**, 3124–3135
28. Lee, Y. K., Choi, I. S., Kim, Y. H., Kim, K. H., Nam, S. Y., Yun, Y. W., *et al.* (2009) Neurite outgrowth effect of 4-O-methylhonokiol by induction of neurotrophic factors through ERK activation. *Neurochem. Res.* **34**, 2251–2260
29. Tang, C., Wang, M., Wang, P., Wang, L., Wu, Q., and Guo, W. (2019) Neural stem cells behave as a functional niche for the maturation of newborn neurons through the secretion of PTN. *Neuron* **101**, 32–44.e36
30. Nikolakopoulou, A. M., Montagne, A., Kisler, K., Dai, Z., Wang, Y., Huuskonen, M. T., *et al.* (2019) Pericyte loss leads to circulatory failure and pleiotrophin depletion causing neuron loss. *Nat. Neurosci.* **22**, 1089–1098
31. Wang, S., Xue, F., Li, W., Shan, Y., Gu, X., Shen, J., *et al.* (2020) Increased expression of Triad1 is associated with neuronal apoptosis after intracerebral hemorrhage in adult rats. *Int. J. Neurosci.* **130**, 759–769
32. Wang, H., Bei, L., Shah, C. A., Huang, W., Platanias, L. C., and Eklund, E. A. (2018) The E3 ubiquitin ligase Triad1 influences development of Mll-Ell-induced acute myeloid leukemia. *Oncogene* **37**, 2532–2544
33. Lee, J., An, S., Choi, Y. M., Jung, J. H., Li, L., Meng, H., *et al.* (2017) TRIAD1 is a novel transcriptional target of p53 and regulates nutlin-3a-induced cell death. *J. Cell Biochem.* **118**, 1733–1740

34. Bae, S., Jung, J. H., An, I. S., Kim, O. Y., Lee, M. J., Lee, J. H., *et al.* (2012) TRIAD1 is negatively regulated by the MDM2 E3 ligase. *Oncol. Rep.* **28**, 1924–1928
35. Li, D., Zhang, J., Huang, W., Jin, H., Shen, A., Yang, L., *et al.* (2013) Up-regulation of Smurf1 after spinal cord injury in adult rats. *J. Mol. Histol.* **44**, 381–390
36. Shimizu, S., Abt, A., and Meucci, O. (2011) Bilaminar co-culture of primary rat cortical neurons and glia. *J. Vis. Exp.* **12**, 3257
37. Guizzetti, M., Moore, N. H., Giordano, G., and Costa, L. G. (2008) Modulation of neuritogenesis by astrocyte muscarinic receptors. *J. Biol. Chem.* **283**, 31884–31897
38. Wang, J., Li, H., Yao, Y., Ren, Y., Lin, J., Hu, J., *et al.* (2018) Beta-elemene enhances GAP-43 expression and neurite outgrowth by inhibiting RhoA kinase activation in rats with spinal cord injury. *Neuroscience* **383**, 12–21
39. Guo, M. M., Qu, S. B., Lu, H. L., Wang, W. B., He, M. L., Su, J. L., *et al.* (2021) Biochanin A alleviates cerebral ischemia/reperfusion injury by suppressing endoplasmic reticulum stress-induced apoptosis and p38MAPK signaling pathway *in vivo* and *in vitro*. *Front. Endocrinol.* **12**, 646720
40. Wang, C., Wang, Q., Lou, Y., Xu, J., Feng, Z., Chen, Y., *et al.* (2018) Salidroside attenuates neuroinflammation and improves functional recovery after spinal cord injury through microglia polarization regulation. *J. Cell Mol. Med.* **22**, 1148–1166
41. Basso, D. M., Beattie, M. S., and Bresnahan, J. C. (1995) A sensitive and reliable locomotor rating scale for open field testing in rats. *J. Neurotrauma* **12**, 1–21
42. Wang, D., Chen, F., Fang, B., Zhang, Z., Dong, Y., Tong, X., *et al.* (2020) MiR-128-3p alleviates spinal cord ischemia/reperfusion injury associated neuroinflammation and cellular apoptosis *via* SP1 suppression in rat. *Front. Neurosci.* **14**, 609613
43. Wang, C., Xu, T., Lachance, B. B., Zhong, X., Shen, G., Xu, T., *et al.* (2021) Critical roles of sphingosine kinase 1 in the regulation of neuroinflammation and neuronal injury after spinal cord injury. *J. Neuroinflam.* **18**, 50
44. Wang, Z., Kang, W., Li, O., Qi, F., Wang, J., You, Y., *et al.* (2021) Abrogation of USP7 is an alternative strategy to downregulate PD-L1 and sensitize gastric cancer cells to T cells killing. *Acta Pharm. Sin B* **11**, 694–707